RESEARCH PAPER



Aerosol impaction-driven assembly produces evenly dispersed nanoparticle coating on polymeric water treatment membranes

Ariel J. Atkinson • Yuqiang Bi • Peter Firth • Omar Alrehaili • Paul Westerhoff • Zachary C. Holman •

Received: 11 October 2019 / Accepted: 12 March 2020 © Springer Nature B.V. 2020

Abstract Nano-enabled water treatment membranes are finding new applications and commercial opportunities, but the commonly used methods for embedding or coating the membranes with nanoparticles have limitations. There is an increasing need for controllable and high-throughput methods for applying nanoparticles uniformly across membrane surfaces in ways that preserve their unique nano-properties while assuring stable attachment. We demonstrate proof-of-concept for the use of aerosol impaction-driven assembly (AIDA) to coat polymeric water treatment membranes. AIDA is a dry-coating technique that has been demonstrated on other substrates. It involves using a pressure differential

This article is part of the topical collection: Nanotechnology Convergence in Africa, Guest Editors: Mamadou Diallo, Abdessattar Abdelkefi, and Bhekie Mamba

Electronic supplementary material The online version of this article (https://doi.org/10.1007/s11051-020-04814-w) contains supplementary material, which is available to authorized users.

A. J. Atkinson (

) Y. Bi O. Alrehaili P. Westerhoff
NSF Nanosystems Engineering Research Center for
Nanotechnology-Enabled Water Treatment (NEWT), School of
Sustainable Engineering and the Built Environment, Arizona State
University, Tempe, AZ 85287, USA
e-mail: Ariel.Atkinson@snwa.com

P. Firth · Z. C. Holman School of Electrical, Computer, and Energy Engineering, Arizona State University, Tempe, AZ 85287, USA

P. Firth · Z. C. Holman (△) Swift Coat, 8501 W. Foothill Dr., Peoria, AZ 85383, USA e-mail: Zachary.Holman@asu.edu

Published online: 29 April 2020

to accelerate aerosolized (premade or in situ-formed) nanoparticles onto a moving sample. The nanoparticles stick by chemical bonding or van der Waals interactions. To provide a proof-of-concept and comparison with other techniques, PVDF membranes with 0.1 µm pore size were coated with functionalized 50-nm-diameter silver and gold nanoparticles using AIDA, spray-coating, and in situ synthesis, and then were characterized. The AIDA coating method produces controllable (i.e., proportional to deposition time) loadings of evenly dispersed, non-agglomerated nanoparticles on the membrane. The method is relatively agnostic to nanoparticle type. The loading efficiency varies with the surface functionality of the nanoparticles, but not their elemental composition. The method has no substantial effect on water flux and produces stable coatings with low nanoparticle release. The AIDA nanoparticle coating method is shown to have inherent flexibility, controllability, and other major advantages (i.e., dispersion, stability) in the quality of the coatings produced.

Keywords Surface modification · Coating techniques · Water treatment · Nanofiltration

Introduction

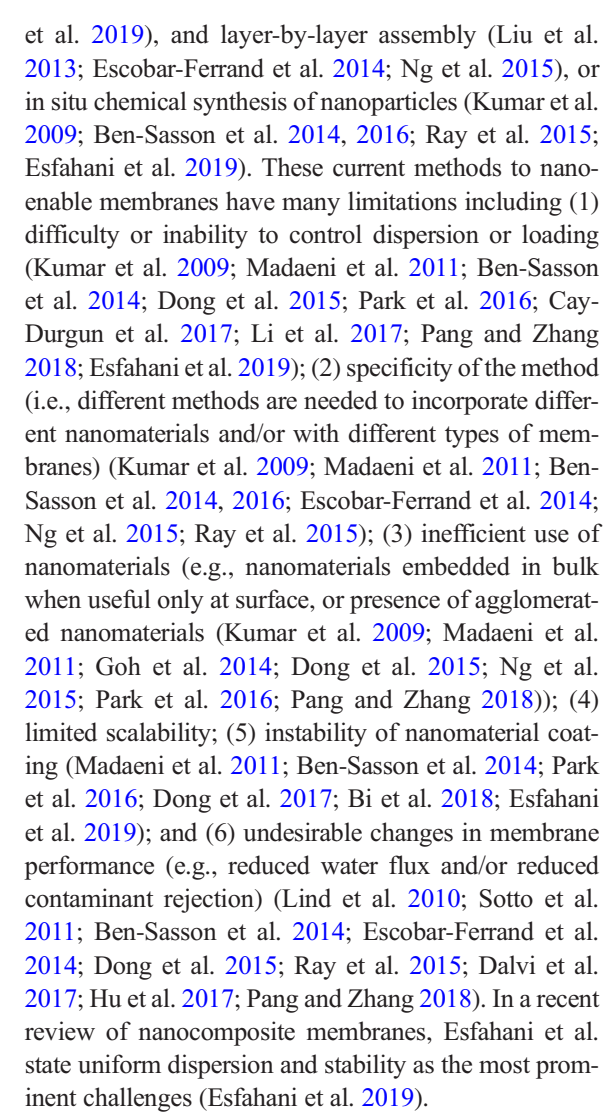
Attaching nanomaterials—including silver (Liu et al. 2013, 2015; Ben-Sasson et al. 2014; Huang et al. 2016; Park et al. 2016; Dong et al. 2017; Bi et al. 2018), gold (Kumar et al. 2009; Ray et al. 2015), zeolites (Lind et al. 2010; Pendergast et al. 2013; Dong et al.



102 Page 2 of 11 J Nanopart Res (2020) 22:102

2015; Cay-Durgun et al. 2017), carbon nanotubes (Vatanpour et al. 2011; Duan et al. 2017; Dudchenko et al. 2017; Zhou et al. 2018), carbon black (Dongare et al. 2017), carbon dots (Li et al. 2017), graphene oxide (Ray et al. 2015), copper (Ben-Sasson et al. 2016), iron oxide (Ng et al. 2015), silica (Jin et al. 2012; Escobar-Ferrand et al. 2014; Dalvi et al. 2017; Pang and Zhang 2018), and titanium dioxide (Madaeni et al. 2011; Sotto et al. 2011; Dalvi et al. 2017)—onto the surface of water treatment membranes or embedding them within their bulk can impart useful functionality. In particular, the nanomaterials can increase water flux (Lind et al. 2010; Pendergast et al. 2013; Dong et al. 2015; Cay-Durgun et al. 2017; Dongare et al. 2017; Dudchenko et al. 2017; Li et al. 2017; Zhou et al. 2018), improve contaminant rejection (Pendergast et al. 2013; Pang and Zhang 2018), prevent fouling (biological, organic, or inorganic) (Madaeni et al. 2011; Vatanpour et al. 2011; Liu et al. 2013, 2015; Ben-Sasson et al. 2014, 2016; Dudchenko et al. 2014; Ng et al. 2015; Park et al. 2016; Dong et al. 2017), or otherwise alter the membrane properties (e.g., electrical conductance (Duan et al. 2017), photonic heating (Ray et al. 2015; Dongare et al. 2017), joule heating (Dudchenko et al. 2017), selective rejection/ passage (Duan et al. 2017; Li et al. 2017)). Research on nano-enabled membranes has been aimed at a range of applications, including wastewater treatment, desalination, high-purity water production, and oil and gas separations, using reverse osmosis, forward osmosis, membrane distillation, and dialysis. As the potential applications expand and nano-enabled membranes are commercialized, there is increasing need for controllable and high-throughput methods for applying nanoparticles uniformly across membrane surfaces while taking advantage of their unique properties.

Common methods for coating or embedding membranes with nanoparticles include attachment of premade nanoparticles using dip coating (Madaeni et al. 2011; Esfahani et al. 2019), spray-gun coating (Dudchenko et al. 2017; Zhou et al. 2018; Esfahani et al. 2019), grafting/chemical attachment (Madaeni et al. 2011; Liu et al. 2015; Ray et al. 2015; Park et al. 2016), addition during membrane casting (Li et al. 2007, 2017; Lind et al. 2010; Sotto et al. 2011; Vatanpour et al. 2011; Jin et al. 2012; Pendergast et al. 2013; Safarpour et al. 2015; Dong et al. 2015; Duan et al. 2015; Cay-Durgun et al. 2017; Dalvi et al. 2017; Pang and Zhang 2018), direct surface deposition (with or without pressure) (Dongare et al. 2017; Duan et al. 2017; Esfahani



Aerosol impaction-driven assembly (AIDA) is a dryspray coating technology that encompasses a number of techniques described in literature, including hypersonic plasma particle deposition and aerosol deposition (Rao et al. 1997, 1998; Hafiz et al. 2004; Akedo 2006; Moridi et al. 2014; Hanft et al. 2015). AIDA involves accelerating aerosolized (premade or in situ-formed) nanoparticles onto a sample substrate, mounted on a moving stage, via a pressure differential across a nozzle. The process occurs in rough vacuum so that nano-sized particles impact the substrate instead of being deflected around it by collisions with the background gas. The particles stick to the substrate by chemical bonding or van der Waals interactions. We previously showed the scalability and capacity of AIDA to produce uniform coatings on silicon and glass substrates with controllable



J Nanopart Res (2020) 22:102 Page 3 of 11 102

coating thickness (sub-monolayer to > 100 µm) and porosity (3-97%) (Firth and Holman 2018). With a slit-shaped nozzle, these films were deposited on areas as large as 5 in. \times 5 in. with thickness non-uniformities of less than 5%. The AIDA coating method lends itself to scaling up because the spray nozzle is linear and not a point source, and thus, the nozzle can be made longer to coat wider substrates, with few other modifications needed. The versatility of AIDA allows for agnostic deposition of pre-formed nanoparticles (of either a single type or a cocktail) or of nanomaterials made in the same apparatus using plasma or flame synthesis immediately prior to deposition. These attributes demonstrate AIDA as a promising new technique to nano-enable materials, and we show here attachment of Ag and Au model nanoparticles with varying surface functionalizations to polymeric water treatment membranes. Although we use Ag and Au nanoparticles and one membrane type, the AIDA coating method can be applied to any substrate and with any chosen nanoparticle.

The overall aim of this paper is to demonstrate proofof-concept for AIDA as an effective, controllable technique to produce uniform and stable nanoparticle coatings on water treatment membranes. To achieve this aim, the specific objectives of this paper are to (1) characterize coatings of pre-formed nanoparticles deposited using AIDA and compare them against two common techniques (in situ nanoparticle formation and spray-gun coating); (2) demonstrate the ability to control and vary nanoparticle loading on the membranes; (3) evaluate the effect of nanoparticle surface functionalization and elemental composition on loading; (4) quantify the stability and release of AIDA nanoparticle coatings in dead-end performance tests; and (5) determine the effect of AIDA nanoparticle coatings on membrane performance (i.e., water flux). This novel coating method has not previously been applied to membranes.

Materials and methods

Reagents and membranes

Hydrophilic PVDF membranes (Durapore, diameter of 47 mm, pore size of 0.1 μm) were purchased from Millipore (Burlington, MA) and used as the membrane substrate in all experiments. PVDF membranes are a common low-pressure membrane used in water

treatment. Low-pressure membranes are also the more difficult polymeric membrane type to coat with nanoparticles due to larger pore size, and fewer demonstrations of nanoparticle coating of low-pressure water treatment membranes have been completed. Gold nanoparticles were used as a model nanoparticle because they are relatively easy to detect and do not readily dissolve in water. Silver nanoparticles were also tested, as they are one of the most common nanoparticles for coating membranes (Liu et al. 2013, 2015; Ben-Sasson et al. 2014; Goh et al. 2014; Huang et al. 2016; Ong et al. 2016; Park et al. 2016; Dong et al. 2017; Bi et al. 2018) and they more readily dissolve in water, releasing antibacterial Ag+ ions. Experiments with silver thus provided additional insight relevant to nanoparticle type, applicability, and coating stability. To evaluate the effect of nanoparticle surface charge, aqueous NanoXact 50-nm gold nanoparticles functionalized with branched polyethyleneimine (bPEI, cationic), polyethylene glycol (PEG, neutral), or citrate (anionic) in solution, as well as aqueous NanoXact 50-nm silver nanoparticles functionalized with branched polyethyleneimine (bPEI, cationic), were purchased from nanoComposix (San Diego, CA). A table of relevant properties of membranes and nanoparticles is provided in Table 1 in the Supplementary Material. All reagents were of ACS reagent grade or better, were purchased from commercial sources, and were used without additional purification. All solutions were made with lab-prepared ultrapure water (≥ $17.9 \text{ M}\Omega \text{ cm}$).

AIDA apparatus

Figure 1 shows an AIDA apparatus with an exchangeable nanomaterial introduction system. AIDA systems couple an upstream chamber operating at 1 to 100 Torr with a downstream chamber operating at 0.1 to 20 Torr through a slit-shaped nozzle that separates the chambers. To deposit a coating, a nanomaterial is introduced into the upstream chamber as a dry aerosol (i.e., solid particles in gas). The carrier gas with aerosolized nanomaterial is accelerated through the nozzle because of the pressure differential across it. The gas in turn accelerates the nanoparticles through collisions. This results in a linear aerosol jet that expands into the downstream chamber, and the nanoparticles reach velocities in excess of 100 m s⁻¹ because the reduced pressure in that chamber decreases the drag experienced by the nanoparticles from the background gas after it



102 Page 4 of 11 J Nanopart Res (2020) 22:102

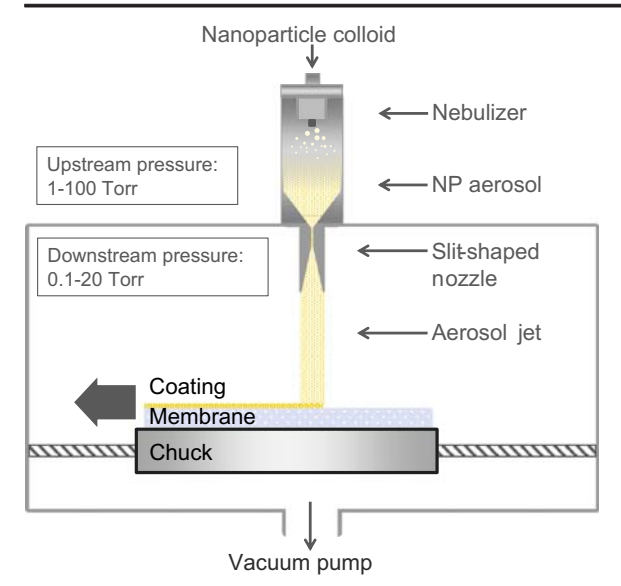


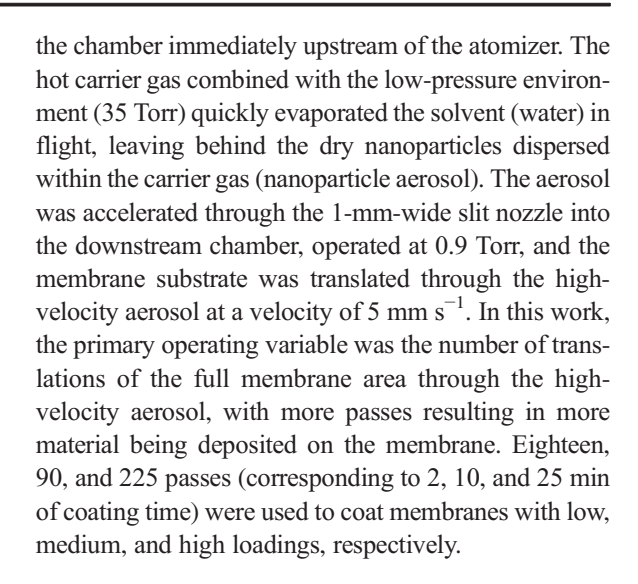
Fig. 1 Aerosol impaction-driven assembly (AIDA) apparatus. A colloidal nanoparticle solution is nebulized in the upstream chamber and dried in flight; the resulting nanoparticles are drawn into the downstream deposition chamber as a linear aerosol jet and deposited onto a translated membrane

slows. A substrate translated through the linear aerosol jet in the downstream chamber is coated with the high-velocity nanomaterial, which sticks by chemical bonding or van der Waals interactions, depending on the deposition velocity and particle and substrate surface chemistry. The final loading of nanoparticles on the membrane is determined by the substrate translation speed and the number of times it passes under the aerosol jet.

Nanoparticle coating

AIDA coating of pre-formed nanoparticles on membranes

Pre-formed gold and silver aqueous nanoparticle solutions (bPEI-Au, citrate-Au, PEG-Au, and bPEI-Ag) at 8.3 μg mL⁻¹ were fed by a liquid flow controller at 0.5 mL min⁻¹ to an ultrasonic atomizer operating at 135 kHz. As the colloidal solution reached the atomizer tip, the vibration produced liquid droplets of the solution with diameters ranging from 500 nm to 2 μ m (as indicated by manufacturer Sonaer Inc.), which corresponds to < 1 nanoparticle to 27 nanoparticles per droplet. The ultrasonic atomizer was affixed to the AIDA system to inject the droplets directly into the upstream chamber. A heated (~100 °C) carrier gas (N₂) was also injected into



Spray-gun coating of pre-formed nanoparticles on membranes

Similar to other spray coating methods in the literature (Dudchenko et al. 2017; Zhou et al. 2018), dispersed nanoparticles were placed in a pressurized chamber and then sprayed from above onto the surface of the membrane. A solution of the cationic gold nanoparticles $(0.05 \text{ mg mL}^{-1})$, the same particles as used in the AIDA coating method, was placed in the chamber of a paint spray-gun (Central Pneumatic Professional, Camarillo, CA). The spray-gun nozzle was placed 7 cm above the membrane surface prior to pressurizing the spray-gun with compressed air. The membrane was sprayed in intervals until all the solution was gone, where each pass over the membrane surface took approximately 10 s and the membrane was allowed to dry for 5 min between each pass. The concentration of nanoparticles deposited on the membrane was intended to be similar to the low loading from the AIDA-coated membranes; subsequent analysis (nanoparticle area by scanning electron microscopy) confirmed this. The membrane was allowed to air-dry for 48 h prior to imaging with the scanning electron microscope.

On-membrane synthesis of gold nanoparticle (in situ) coating

Gold nanoparticles were formed in situ on membranes using a modified method from Kumar et al. (2009) Briefly, the membrane was placed in an Amicon® stirred cell (Millipore, Burlington, MA) with 0.01 M



J Nanopart Res (2020) 22:102 Page 5 of 11 102

HAuCl₄ solution and stirred overnight. The solution was removed, and the membrane was then exposed to 0.1 M NaBH₄ with stirring for 30 min. The concentration of nanoparticles deposited on the membrane was intended to be similar to the high loading from the AIDA-coated membranes; however, subsequent analysis by SEM-BSE showed the surface gold loading was twice that of the AIDA-coated membrane. We observed significant nanoparticle agglomeration in the in situcoated samples. The membrane was allowed to air-dry for 48 h prior to imaging with the scanning electron microscope.

Nanoparticle-coated membrane characterization

Membrane performance and coating stability

Nanoparticle release tests from membranes were performed using a dead-end stirred Amicon® cell (Millipore, Burlington, MA) connected to a pressurized water vessel (Sterlitech, Kent, WA) with 13.4 cm² of active membrane area exposed to the feed. The system was operated at 22.0 °C and with an applied transmembrane pressure of 2.75 bar for ~60 min until 5.0 L of water was filtered. Nanoparticle concentration and size distribution in the retentate and permeate after continuous mixing and filtration were analyzed using a single-particle inductively coupled plasma-mass spectrometry (ICP-MS) method previously used by our group (Bi et al. 2018).

Nanoparticle mass loading on membranes

The nanoparticle mass loading ($\mu g \text{ cm}^{-2}$) on the membranes before and after the performance and coating stability tests was quantified by digesting membrane samples with aqua regia in a microwave-assisted plastic digestion procedure and measuring gold or silver concentration with ICP-MS as further described in the Supplementary Material.

Nanoparticle size and aerial dispersion on membranes

The size and aerial dispersion of nanoparticles on the surface of the coated membranes were analyzed with an FEI XL30 scanning electron microscope (SEM) (Hillsboro, OR) with secondary electron (SE), backscattered electron (BSE), and energy dispersive x-ray (EDX) detectors. Quantitative techniques to analyze the BSE

images of nano-enabled membranes, including the construction of effective particle/agglomerate size distributions and nearest-neighbor distance (NND) cumulative distribution functions (CDFs), were developed. The BSE images were analyzed using Image J64 software (NIH provided public domain Java image processing software) (Rasband 2013). Distances between all particles in the images were calculated using their *x*- and *y*-coordinates. For each particle, the minimum distance to another particle was considered its nearest-neighbor distance.

Results and discussion

Aerial dispersion of nanoparticles

Figure 2 a-c show that nanoparticles on the AIDAcoated membranes were evenly dispersed and deposited as individual, non-agglomerated nanoparticles that maintained their shape during AIDA coating. Figure 2 d and e show that, with two common nanoparticle coating methods, spray-gun coating and in situ coating, the nanoparticles were either aggregated in specific regions (potentially associated with deposited droplets) or agglomerated (i.e., not evenly distributed as single nanoparticles across the membrane). Because aggregation and agglomeration likely reduce the efficacy of the nanoparticle coating during use, the even dispersion of single nanoparticles is a major advantage of the AIDA coating technique. Though dispersion, aggregation, and agglomeration on nanoparticle coated membranes are rarely reported or evaluated quantitatively in the literature, there are some reports that show nanoparticles do commonly agglomerate or aggregate when added to membranes using in situ nanoparticle coating (Kumar et al. 2009), addition during membrane casting (Li et al. 2007, 2017; Dong et al. 2015; Cay-Durgun et al. 2017), or dip coating (Madaeni et al. 2011).

Effective particle/agglomerate size distributions, compiled from the SEM-BSE images, indicate whether nanoparticles are agglomerated. Figure 3 shows that the size frequency distribution of particles on AIDA-coated membranes had a mean of 53 ± 1 nm with a polydispersity of 0.1. The size distributions of nanoparticles on the coated membrane were similar to those in the solution used for AIDA coating, demonstrating that the nanoparticles were unchanged in size during the AIDA coating process. Figure 3 also shows that the particles on the spray-gun-coated



102 Page 6 of 11 J Nanopart Res (2020) 22:102

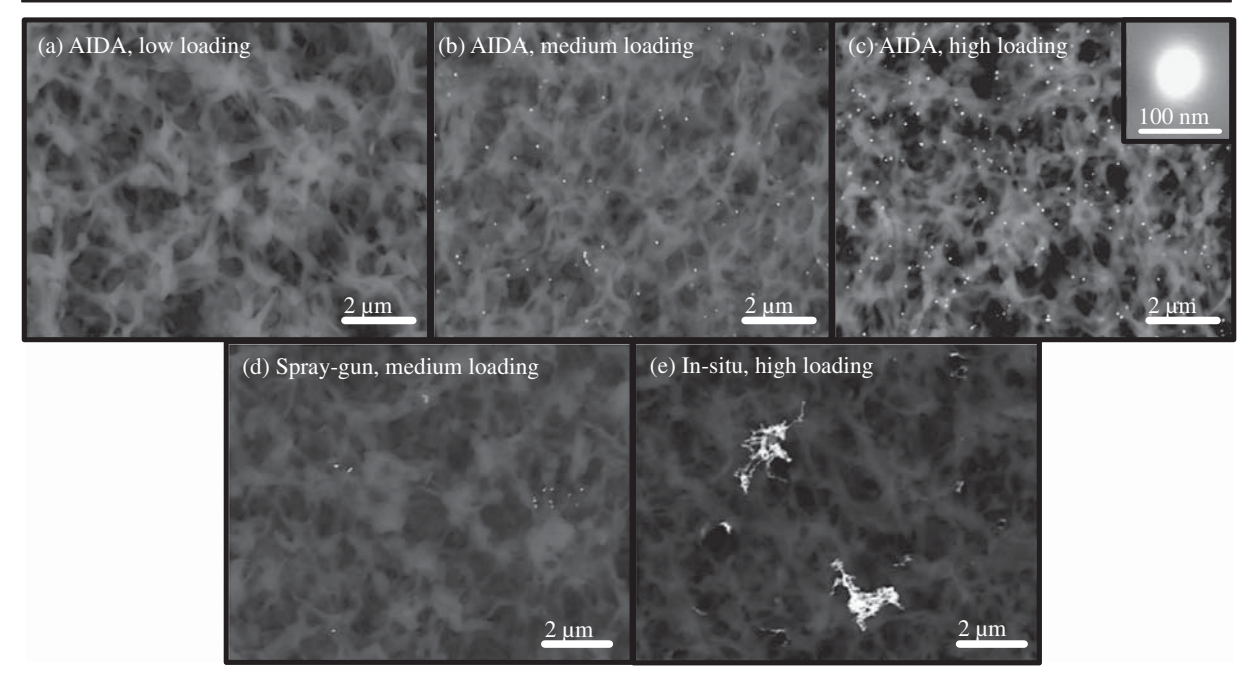


Fig. 2 SEM-BSE images of membranes coated with gold nanoparticles using: AIDA to achieve low (18 passes) to high (225 passes) loadings (**a**–**c**), a spray-gun (**d**), and on-membrane in situ

synthesis (e). Inset in ${\bf c}$ shows a single nanoparticle at \times 20 higher magnification

membranes had a similar mean size of 50 nm but a polydispersity of 0.3 due to a few particles with diameters twice or three times their in-solution size (i.e., 100 or 150 nm). The nanoparticle size distributions of the AIDA-coated and spray-gun-coated membranes were not statistically different (p = 0.13). Finally, Fig. 3 shows that the size of nanoparticles on the in situ–coated membrane varied more than with either spray methods, with some small particles (diameter < 20 nm) but also very large agglomerates up to 1.5 μ m in diameter. The in situ nanoparticle formation was expected to produce single gold nanoparticles on the order of 10 nm in diameter (Kumar et al. 2009), but the mean particle size was 153 nm with a polydispersity of 3.8. There was clear and substantial agglomeration of nanoparticles with this method.

Nearest-neighbor distance (NND) cumulative distribution functions (CDFs) were constructed for particles and agglomerates on each coated membrane (Figs. 4 and 6 in the Supplementary Material). When the NND CDFs of the coated membranes deviate significantly from the reference NND CDFs (corresponding to randomly dispersed particles with the same total areal concentration), this indicates the nanoparticles are not well dispersed across the membrane. The NND CDFs of the AIDA-coated membranes (Figs. 4a and 6 in the Supplementary

Material) are nearly the same (p > 0.05) as randomly dispersed particles, indicating that the AIDA coating method produced membranes with evenly dispersed nanoparticles on the surface. Figure 4 b and c show that the NND CDFs of the spray-gun-coated and in situ-coated membranes are statistically different from the reference NND CDFs (p < 0.05). Additional discussion of NND CDFs is given in the Supplementary Material Section A2.1. The NNDs of almost all nanoparticles were lower than the 95% confidence intervals for the spray-gun-coated and in situ-coated membranes, indicating that the nanoparticles aggregated when they were coated onto the membranes.

Controllable nanoparticle mass loading with AIDA

The images in Fig. 2a–c reveal that nanoparticle loading (μg cm⁻²) on membranes increases with the number of passes of the membrane under the aerosol jet during AIDA deposition. Further, we found that gold nanoparticle mass loading (as measured by digestion-ICP-MS) was linearly and statistically correlated (p < 0.05) with the number of passes, and thus the deposition time (Supplementary Material Fig. 7). The nanoparticle loadings achieved by AIDA (0.15 to 0.60 μg cm⁻²) are comparable



J Nanopart Res (2020) 22:102 Page 7 of 11 102

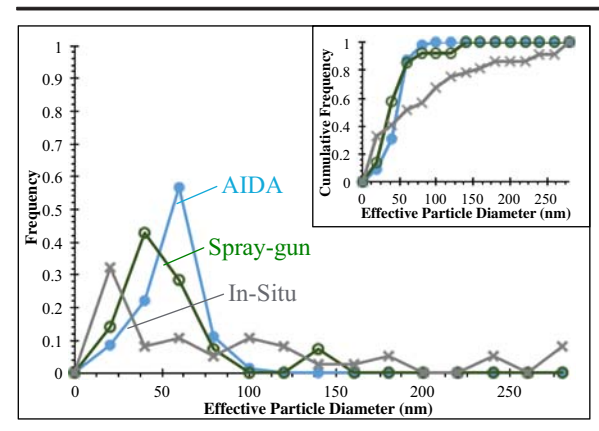


Fig. 3 Effective nanoparticle/agglomerate size distribution on AIDA-coated membrane (\bullet , medium loading, n = 81 particles), spray-gun-coated membrane (\bullet , n = 14 particles), and in situcoated membrane (\bullet , n = 37 particles). Inset is the cumulative size distribution for each of the membranes. Nanoparticle sizes calculated from SEM-BSE images

with those produced by other methods at levels required to meet their intended application (Kumar et al. 2009; Sotto et al. 2011; Madaeni et al. 2011; Liu et al. 2013; Ben-Sasson et al. 2014; Dong et al. 2015; Park et al. 2016; Huang et al. 2016; Cay-Durgun et al. 2017; Li et al. 2017; Bi et al. 2018; Pang and Zhang 2018). However, other techniques do not offer the same easy and independent loading tunability enabled by AIDA. For example, grafting of nanoparticles and in situ nanoparticle formation can be difficult to control because they require varying the ratio and concentration of reactants and they rely on the ability to predict yield of chemical reactions under varying conditions (Kumar et al. 2009; Sotto et al. 2011; Madaeni et al. 2011; Liu et al. 2013; Ben-Sasson et al. 2014; Dong et al. 2015; Park et al. 2016; Huang et al. 2016; Cay-Durgun et al. 2017; Li et al. 2017; Bi et al. 2018; Pang and Zhang 2018).

The drawback of the present work is that the deposition efficiency for the AIDA coatings was only 2%, calculated as the mass of gold on the membrane divided by the mass of colloidal gold introduced into the tool. However, no attempts to improve this efficiency were made on the prototype AIDA device. With other (noncolloidal) nanoparticles and AIDA protocols, we have measured deposition efficiencies greater than 70% (Firth and Holman 2018). This lower efficiency could be due to nanoparticles going through the membrane without sticking to the surface/within the membrane depth or the nanoparticles not reaching the membrane surface. Particles that do not reach the substrate are lost

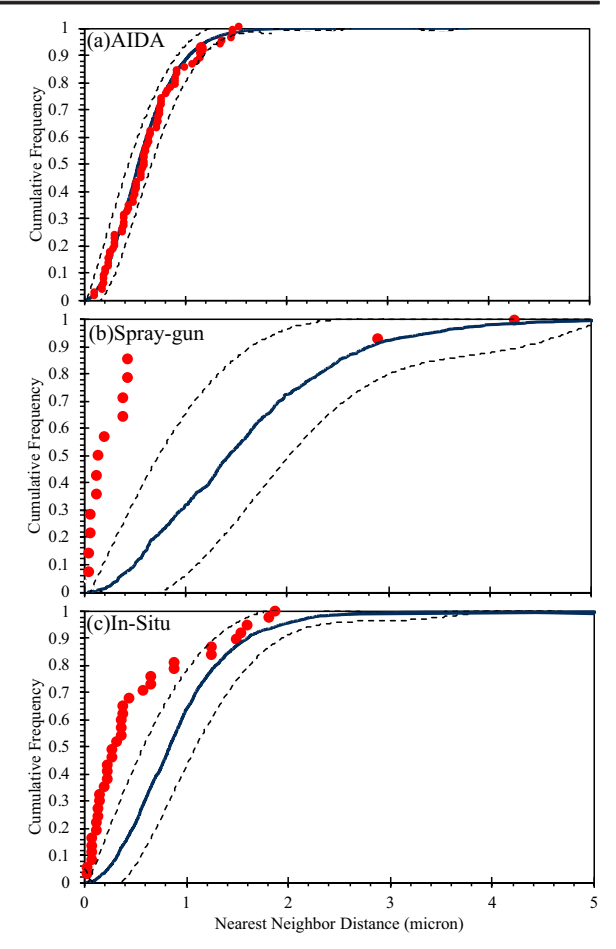


Fig. 4 Nearest-neighbor distance (NND) cumulative distribution functions (CDFs) for a AIDA-coated membrane (medium loading, n=81 particles), **b** spray-gun-coated membrane (n=14 particles), and **c** in situ-coated membrane (n=37 particles). Red circles correspond to sample data, dark blue lines correspond to the reference NND CDFs for randomly dispersed particles having the same total loading, and black dashed lines correspond to the 95% confidence intervals for the reference NND CDFs. NNDs calculated from SEM-BSE images

to the walls of the vacuum chamber in flight between where the aerosol is generated and deposition on the substrate occurs. As much higher efficiency has been observed when depositing nanoparticles synthesized in flight from a gas using a plasma (no liquids), this indicates the primary loss mechanism is via liquid droplets hitting the chamber walls. Future steps to increase efficiency will thus focus on coupling enough thermal energy into the system to fully evaporate the solvent of liquid droplets in-flight before the droplets encounter a chamber wall. As the technology is scaled up, optimizing the deposition efficiency, specifically the



102 Page 8 of 11 J Nanopart Res (2020) 22:102

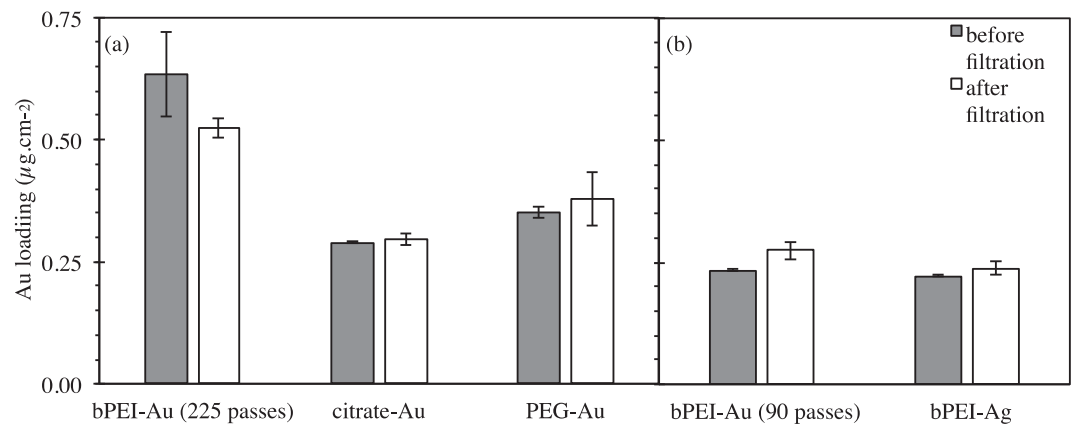


Fig. 5 Gold or silver mass loading on AIDA-coated membranes before and after dead-end performance testing using three types of 50-nm-diameter gold nanoparticles and one type of 50-nm-diameter silver nanoparticle. a Citrate-Au, PEG-Au, and bPEI-Au were coated with the same number of passes (225 passes) and colloidal nanoparticle concentration, but the gold mass loadings measured are statistically different (p < 0.05). b bPEI-Au and

bPEI-Ag were coated with the same number of passes (90 passes) and colloidal nanoparticle concentration and had statistically the same mass loading (p > 0.05). Gold and silver mass loading was measured using digestion-ICP-MS. Error bars represent one standard deviation (n = 3-6). In the case of duplicates (n = 2), the error bar represents the range

aerosolization process, of colloidal nanoparticles will be an area of focus, as well as depositing on membranes with different properties including more dense membranes.

Effect of nanoparticle surface functionalization and elemental composition on AIDA coatings

Gold nanoparticles with different surface functionalizations were coated with AIDA onto membranes, and Fig. 5a indicates statistical differences (p < 0.05) in the resulting gold loadings for nominally identical deposition conditions. The loading was highest with branched polyethyleneimine-coated (bPEI-Au) nanoparticles, followed by polyethylene-glycol-coated (PEG-Au) nanoparticles and citrate-coated (citrate-Au) nanoparticles. Nanoparticle characteristics are provided in Supplementary Material Table 1. The gold loadings correlated with zeta potential (at the same pH). The positively charged bPEI-Au nanoparticles led to a gold loading nearly twice that of the negatively charged citrate-Au nanoparticles. Therefore, we suspect that electrostatic interactions with the negatively charged PVDF membrane (zeta potential = -14 mV at pH 7) and particle charge-dependent losses upstream of the membrane are the dominant factors in nanoparticle deposition and retention on the membrane during AIDA coating shown here.

Figure 5 b shows the AIDA process is also not impacted by nanoparticle elemental composition. Using

the same AIDA deposition parameters, coating with bPEI-Au and bPEI-Ag nanoparticles resulted in membranes with statistically (p > 0.05) the same nanoparticle loading. This result demonstrates that AIDA as a method is independent of the material, relatively agnostic to nanoparticle characteristics, and that nanoparticle loading is consistent when using the same operating parameters.

Other methods described in the literature typically explore coating or embedding only one type of nanoparticle (i.e., a particular elemental composition of the nanoparticles or a nanoparticle with a particular surface functionalization), and the effect of nanoparticle functionalization and elemental composition on coating efficiency has not been thoroughly and systematically compared. We showed that AIDA is agnostic to elemental composition of nanoparticles, although surface functionalization can affect coating efficiency. However, this effect could potentially be less than with other coating methods that rely on chemical reactions or bonding with nanoparticle surface functional groups. AIDA is a dry deposition method that does not require specific surface functionalization for attachment.

Water flux of AIDA-coated membranes

It is typical to observe, when membranes are nanoenabled or otherwise modified, a modest change in water flux due to the additional resistance from



J Nanopart Res (2020) 22:102 Page 9 of 11 102

nanoparticles or structures, blocking of existing defects, and reduced surface area for water flux (Ben-Sasson et al. 2014; Goh et al. 2014; Ong et al. 2016). The initial water flux of all coated membranes was within 10% of the initial water flux of the virgin uncoated membranes. Figure 8 (in the Supplementary Material) shows some variability in normalized water flux over time among the AIDA-coated membranes, and there are a few time points at which the water flux was statistically different (both higher and lower) from the uncoated membranes. This is discussed in greater detail in Supplementary Material Section A2.2. However, the normalized water flux in coated membranes was not statistically different from that of the uncoated control membranes for the majority of the measured points over time.

Release of nanoparticles from AIDA-coated membranes

Nanoparticle release depends on many factors, including method of nanoparticle coating, nanoparticle type and properties, membrane type, and the release test used. Nanoparticle release values have been reported to range from less than 1 to 90% of the initial nanoparticle loading on the membrane (Diagne et al. 2012; Ben-Sasson et al. 2014; Liu et al. 2015; Dong et al. 2017; Hu et al. 2017; Jahan et al. 2017; Bi et al. 2018). Figure 5 illustrates nanoparticle loading on the AIDA-coated membranes before and after passing 5 L of water through them over 1 h of operation. There were no statistical differences (p > 0.05) in mass loadings before and after the use test; nanoparticle release from AIDAcoated membranes was lower than or similar to what is reported with other nanoparticle coating techniques (Diagne et al. 2012; Ben-Sasson et al. 2014; Liu et al. 2015; Dong et al. 2017; Hu et al. 2017; Jahan et al. 2017; Bi et al. 2018). No nanoparticles or dissolved metals were detected in the retentates, and less than 5% of gold or silver was released from the membrane into the permeate (cumulative release data shown in Fig. 9 in the Supplementary Material), despite the pore size of the membranes (100 nm) being larger than the nanoparticle size (50 nm). Most of the metal release occurred in the first 10 mL of water filtered for all membranes, and no additional significant release (< 1%, <5 ng) was observed after 2.5 min of operation. The total metal concentration measured in the first permeate samples collected ranged from 72 to 275 ng L^{-1} and quickly dropped to below 10 ng L⁻¹ in subsequent permeate samples. This release trend (i.e., high release in the initial operation and low or no release thereafter) is consistent with other nano-impregnated membranes in the literature, which have demonstrated the most stable attachment (Diagne et al. 2012; Ben-Sasson et al. 2014; Liu et al. 2015; Park et al. 2016; Dong et al. 2017; Hu et al. 2017; Jahan et al. 2017; Bi et al. 2018). There are no regulations for gold in drinking water, but silver has a non-enforceable secondary drinking water standard of 0.1 mg L⁻¹(EPA 2003). In the present experiments, the dissolved silver concentration in the permeate was always many orders of magnitude lower than this secondary standard.

The mechanism (i.e., dissolution vs. detachment) of nanoparticle release has important implications for stability (i.e., stable nanoparticles vs. stable attachment), but is also important for applicability (e.g., silver is expected to and needs to dissolve to be effective at inactivating bacteria (Xiu et al. 2012)). The silver released into the permeate from the membrane coated with bPEI-Ag nanoparticles was mostly $(91 \pm 3\%)$ in the dissolved form. This result is desired for the applicability of silver-AIDA-coated membranes, and it is also good from a stability perspective as it indicates that dissolution, and not detachment, was the major release mechanism. With the gold-coated membranes, there was no dissolved gold observed in the permeates; the small amount of gold released was nanoparticles with size equivalent to that of the Au nanoparticles loaded onto the membrane. A representative time-resolved analysis spectrum from single particle ICP-MS and corresponding size distribution of gold nanoparticles released into the permeate from the bPEI-Au-coated membrane are given in Fig. 10 in the Supplementary Material. The mean diameter of the released gold nanoparticles was 52 ± 7.4 nm, consistent with the nanoparticle size in solution prior to coating. The unaltered nanoparticle size demonstrates that the gold nanoparticles, unlike the silver nanoparticles, did not dissolve and were instead released into the permeate as entire particles. This also confirms that the gold nanoparticles remained intact during AIDA coating.

Implications

This manuscript demonstrates proof-of-concept for the AIDA coating method of polymeric water treatment membranes. Additionally, this work demonstrates that the AIDA coating method has advantages over most other nanoparticle coating methods for water treatment



102 Page 10 of 11 J Nanopart Res (2020) 22:102

membranes, including controllable nanoparticle loading, evenly dispersed non-aggregated/agglomerated nanoparticles on membranes, relative agnosticism to nanoparticle elemental composition and surface functionality, and excellent coating stability during use (i.e., with low nanoparticle release). Future work with the AIDA coating method may include using nanoparticle cocktails to impart multifunctionality to membranes, improving coating yield, coating different types of membranes (e.g., varied materials, properties, and configurations), and scaling up the apparatus and coating method.

Acknowledgments Laurel Passantino provided technical editing.

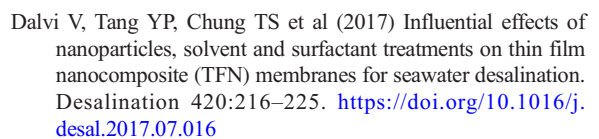
Funding information This work was partially funded by the National Science Foundation Nanosystems Engineering Research Center on Nanotechnology-Enabled Water Treatment (NEWT) Cooperative Agreement ERC-1449500, the Engineering Research Center Program of the National Science Foundation and the Office of Energy Efficiency and Renewable Energy of the Department of Energy under NSF Cooperative Agreement EEC-1041895, and the US Environmental Protection Agency through the STAR program (RD83558001).

Compliance with ethical standards

Conflict of interest The authors declare that they have no conflict of interest.

References

- Akedo J (2006) Aerosol deposition of ceramic thick films at room temperature: densification mechanism of ceramic layers. In:
 Journal of the American Ceramic Society, pp 1834–1839
- Ben-Sasson M, Lu X, Bar-Zeev E, Zodrow KR, Nejati S, Qi G, Giannelis EP, Elimelech M (2014) In situ formation of silver nanoparticles on thin-film composite reverse osmosis membranes for biofouling mitigation. Water Res 62:260–270. https://doi.org/10.1016/j.watres.2014.05.049
- Ben-Sasson M, Lu X, Nejati S et al (2016) In situ surface functionalization of reverse osmosis membranes with biocidal copper nanoparticles. Desalination 388:1–8. https://doi. org/10.1016/j.desal.2016.03.005
- Bi Y, Han B, Zimmerman S, Perreault F, Sinha S, Westerhoff P (2018) Four release tests exhibit variable silver stability from nanoparticle-modified reverse osmosis membranes. Water Res 143:77–86. https://doi.org/10.1016/j.watres.2018.06.036
- Cay-Durgun P, McCloskey C, Konecny J et al (2017) Evaluation of thin film nanocomposite reverse osmosis membranes for long-term brackish water desalination performance. Desalination 404:304–312. https://doi.org/10.1016/j. desal.2016.10.014



- Diagne F, Malaisamy R, Boddie V et al (2012) Polyelectrolyte and silver nanoparticle modification of microfiltration membranes to mitigate organic and bacterial fouling. Environ Sci Technol 46:4025–4033. https://doi.org/10.1021/es203945v
- Dong C, Wang Z, Wu J et al (2017) A green strategy to immobilize silver nanoparticles onto reverse osmosis membrane for enhanced anti-biofouling property. Desalination 401:32–41. https://doi.org/10.1016/j.desal.2016.06.034
- Dong H, Zhao L, Zhang L et al (2015) High-flux reverse osmosis membranes incorporated with NaY zeolite nanoparticles for brackish water desalination. J Membr Sci 476:373–383. https://doi.org/10.1016/j.memsci.2014.11.054
- Dongare PD, Alabastri A, Pedersen S, Zodrow KR, Hogan NJ, Neumann O, Wu J, Wang T, Deshmukh A, Elimelech M, Li Q, Nordlander P, Halas NJ (2017) Nanophotonics-enabled solar membrane distillation for off-grid water purification. Proc Natl Acad Sci 114:6936–6941. https://doi.org/10.1073/pnas.1701835114
- Duan J, Litwiller E, Pinnau I (2015) Preparation and water desalination properties of POSS-polyamide nanocomposite reverse osmosis membranes. J Membr Sci 473:157–164. https://doi.org/10.1016/j.memsci.2014.09.022
- Duan W, Chen G, Chen C et al (2017) Electrochemical removal of hexavalent chromium using electrically conducting carbon nanotube/polymer composite ultrafiltration membranes. J Membr Sci 531:160–171. https://doi.org/10.1016/j. memsci.2017.02.050
- Dudchenko AV, Chen C, Cardenas A, Rolf J, Jassby D (2017) Frequency-dependent stability of CNT Joule heaters in ionizable media and desalination processes. Nat Nanotechnol 12:557–563. https://doi.org/10.1038/nnano.2017.102
- Dudchenko AV, Rolf J, Russell K et al (2014) Organic fouling inhibition on electrically conducting carbon nanotube-polyvinyl alcohol composite ultrafiltration membranes. J Membr Sci 468: 1–10. https://doi.org/10.1016/j.memsci.2014.05.041
- US EPA (2003) National Secondary Drinking Water Regulations Escobar-Ferrand L, Li D, Lee D, Durning CJ (2014) Allnanoparticle layer-by-layer surface modification of microand ultrafiltration membranes. Langmuir 30:5545–5556. https://doi.org/10.1021/la5002489
- Esfahani MR, Aktij SA, Dabaghian Z et al (2019) Nanocomposite membranes for water separation and purification: fabrication , modification , and applications. Sep Purif Technol 213:465–499. https://doi.org/10.1016/j.seppur.2018.12.050
- Firth P, Holman ZC (2018) Aerosol impaction-driven assembly system for production of uniform nanoparticle thin films with independently tunable thickness and porosity. ACS Appl Nano Mater 1:4351–4357. https://doi.org/10.1021/acsanm.8b01334
- Goh PS, Ng BC, Lau WJ, Ismail AF (2014) Inorganic nanomaterials in polymeric ultrafiltration membranes for water treatment. Sep Purif Rev 2119:140715103711008. https://doi.org/10.1080/15422119.2014.926274
- Hafiz J, Wang X, Mukherjee R et al (2004) Hypersonic plasma particle deposition of Si Ti N nanostructured coatings. Surf CoatingTechnol 189:364–370. https://doi.org/10.1016/j.surfcoat.2004.08.226



J Nanopart Res (2020) 22:102 Page 11 of 11 102

Hanft D, Exner J, Schubert M et al (2015) An overview of the aerosol deposition method: process fundamentals and new trends in materials applications. J Ceram Sci Technol 6:147– 181. https://doi.org/10.4416/JCST2015-00018

- Hu M, Zhong K, Liang Y et al (2017) Effects of particle morphology on the antibiofouling performance of silver embedded polysulfone membranes and rate of silver leaching. Ind Eng Chem Res 56:2240–2246. https://doi.org/10.1021/acs.iecr.6 b04934
- Huang L, Zhao S, Wang Z et al (2016) In situ immobilization of silver nanoparticles for improving permeability, antifouling and anti-bacterial properties of ultrafiltration membrane. J Membr Sci 499:269–281. https://doi.org/10.1016/j. memsci.2015.10.055
- Jahan S, Alias YB, Abu Bakar Bin AF, Yusoff Bin I (2017) Ionic release behavior of polymer-coated and uncoated metal nanoparticles (MNPs) in various conditions: effects of particle shape, size, and natural media reactivity. Colloid Polym Sci 295:1961–1971. https://doi.org/10.1007/s00396-017-4155-0
- Jin L, Shi W, Yu S et al (2012) Preparation and characterization of a novel PA-SiO2nanofiltration membrane for raw water treatment. Desalination 298:34–41. https://doi.org/10.1016/j. desal.2012.04.024
- Kumar R, Pandey AK, Tyagi AK, Dey GK, Ramagiri SV, Bellare JR, Goswami A (2009) In situ formation of stable gold nanoparticles in polymer inclusion membranes. J Colloid Interface Sci 337:523–530. https://doi.org/10.1016/j. jcis.2009.05.060
- Li Y, Krantz WB, Chung TS (2007) A novel primer to prevent nanoparticle agglomeration in mixed matrix membranes. AIChE 53:2470–2475. https://doi.org/10.1002/aic
- Li Y, Li S, Zhang K (2017) Influence of hydrophilic carbon dots on polyamide thin film nanocomposite reverse osmosis membranes. J Membr Sci 537:42-53. https://doi. org/10.1016/j.memsci.2017.05.026
- Lind ML, Eumine Suk D, Nguyen T-V, Hoek EMV (2010)
 Tailoring the structure of thin film nanocomposite membranes to achieve seawater RO membrane performance.
 Environ Sci Technol 44:8230–8235. https://doi.org/10.1021/es101569p
- Liu S, Fang F, Wu J, Zhang K (2015) The anti-biofouling properties of thin-film composite nanofiltration membranes grafted with biogenic silver nanoparticles. Desalination 375:121–128. https://doi.org/10.1016/j.desal.2015.08.007
- Liu X, Qi S, Li Y, Yang L, Cao B, Tang CY (2013) Synthesis and characterization of novel antibacterial silver nanocomposite nanofiltration and forward osmosis membranes based on layer-by-layer assembly. Water Res 47:3081–3092. https://doi.org/10.1016/j.watres.2013.03.018
- Madaeni SS, Zinadini S, Vatanpour V (2011) A new approach to improve antifouling property of PVDF membrane using in situ polymerization of PAA functionalized TiO2 nanoparticles. J Membr Sci 380:155–162. https://doi.org/10.1016/j. memsci.2011.07.006
- Moridi A, Hassani-Gangaraj S, Guagliano M, Dao M (2014) Cold spray coating: review of material systems and future perspectives. Surf Eng 30:369–395
- Ng QH, Lim JK, Ahmad AL et al (2015) Magnetic nanoparticles augmented composite membranes in removal of organic foulant through magnetic actuation. J Membr Sci 493:134– 146. https://doi.org/10.1016/j.memsci.2015.06.045

- Ong CS, Goh PS, Lau WJ et al (2016) Nanomaterials for biofouling and scaling mitigation of thin film composite membrane: a review. Desalination 393:2–15. https://doi.org/10.1016/j.desal.2016.01.007
- Pang R, Zhang K (2018) Fabrication of hydrophobic fluorinated silica-polyamide thin film nanocomposite reverse osmosis membranes with dramatically improved salt rejection. J Colloid Interface Sci 510:127–132. https://doi.org/10.1016 /j.jcis.2017.09.062
- Park SH, Ko YS, Park SJ et al (2016) Immobilization of silver nanoparticle-decorated silica particles on polyamide thin film composite membranes for antibacterial properties. J Membr Sci 499:80–91. https://doi.org/10.1016/j.memsci.2015.09.060
- Pendergast MM, Ghosh AK, Hoek EMV (2013) Separation performance and interfacial properties of nanocomposite reverse osmosis membranes. Desalination 308:180–185. https://doi. org/10.1016/j.desal.2011.05.005
- Rao NP, Lee HJ, Kelkar M et al (1997) Nanostructured materials production by hypersonic plasma particle deposition. Nanostruct Mater 9:129–132. https://doi.org/10.1016 /S0965-9773(97)00035-4
- Rao NP, Tymiak N, Blum J et al (1998) Hypersonic plasma particle deposition of nanostructured silicon and silicon carbide. J Aerosol Sci 29:707–720. https://doi.org/10.1016 /S0021-8502(97)10015-5
- Rasband W (2013) ImageJ.:2013
- Ray JR, Tadepalli S, Nergiz SZ, Liu KK, You L, Tang Y, Singamaneni S, Jun YS (2015) Hydrophilic, bactericidal nanoheater-enabled reverse osmosis membranes to improve fouling resistance. ACS Appl Mater Interfaces 7:11117– 11126. https://doi.org/10.1021/am509174j
- Safarpour M, Khataee A, Vatanpour V (2015) Thin film nanocomposite reverse osmosis membrane modified by reduced graphene oxide/TiO<inf>2</inf> with improved desalination performance. J Membr Sci 489:43–54. https://doi.org/10.1016/j.memsci.2015.04.010
- Sotto A, Boromand A, Balta S et al (2011) Doping of polyethersulfone nanofiltration membranes: antifouling effect observed at ultralow concentrations of TiO2nanoparticles. J Mater Chem 21:10311–10320. https://doi.org/10.1039/c1 jm11040c
- Vatanpour V, Madaeni SS, Moradian R et al (2011) Fabrication and characterization of novel antifouling nanofiltration membrane prepared from oxidized multiwalled carbon nanotube/polyethersulfone nanocomposite. J Membr Sci 375:284–294. https://doi.org/10.1016/j.memsci.2011.03.055
- Xiu ZM, Zhang QB, Puppala HL, Colvin VL, Alvarez PJ (2012) Negligible particle-specific antibacterial activity of silver nanoparticles. Nano Lett 12:4271–4275. https://doi. org/10.1021/nl301934w
- Zhou Z, Hu Y, Boo C et al (2018) High-performance thin-film composite membrane with an ultrathin spray-coated carbon nanotube interlayer. Environ Sci Technol Lett 5:243–248. https://doi.org/10.1021/acs.estlett.8b00169

Publisher's note Springer Nature remains neutral with regard to jurisdictional claims in published maps and institutional affiliations.

